Dalton Transactions

Accepted Manuscript

ROYAL SOCIETY OF CHEMISTRY

www.rsc.org/dalton

Self-Assembly of Linear [$Mn^{II}_2Mn^{III}$] Units with End-On Azido Bridges: The Construction of Ferromagnetic Chain using S_T = 7 High-Spin Trimers

Yuan Jiang,[a] Lei Qin,[b] Guanghua Li,[a] Ghulam Abbas, [a] Yanqun Cao,[a] Gang Wu,[*,a] Tian Han,[b] Yan-Zhen Zheng[*,b] Shilun Qiu[*,a]

[a] State Key Laboratory of Inorganic Synthesis & Preparative Chemistry, Jilin University, 2699 Qianjin Street, Changchun 130012, China

[b] Centre for Applied Chemical Research, Frontier Institute of Science and Technology, Xi'an Jiaotong University, Xi'an 710054, China

Abstract

The controlled organization of high-spin complexes into 1D coordination polymers is a challenge in molecular magnetism. In this work, we report a ferromagnetic Mn trimer $Mn_3(HL)_2(CH_3OH)_6(Br)_4 \cdot Br \cdot (CH_3OH)_2$ **1** (H_2L = 2-[(9H-fluoren-9-yl)amino] propane-1, 3-diol) with the ground spin state of S_T = 7 that can be assembled into one-dimensional coordination chain $[Mn_3(HL)_2(CH_3OH)_2(Br)_4(N_3)(H_2O) \cdot CH_3OH]_\infty$ **2** using azido bridging ligands. Interestingly, the ferromagnetic nature of **1** is well retained in **2**. However, due to the negligible magnetic anisotropy in **1**, both **1** and **2** do not show slow-relaxation of magnetization, which indicates during the process of molecular assembly not only the intratrimer magnetic interaction but also the magnetic anisotropy of the trimer can be reserved.

Introduction

Since the discovery of single-molecule magnets (SMMs), controlled arrangement of such anisotropic high spin molecules in different dimensions has become a major challenge in the field of molecule-based magnetic materials.[1] These efforts could enhance the intrinsic SMM properties and provide a unique opportunity to investigate new magnetic behaviors at the frontier between SMMs and long-range magnetic ordered materials. [2] For example, weak supramolecular interactions between SMMs could modify their quantum properties and provide new magnetic behaviors. [3] On the other hand, linking SMMs into one-dimensional (1D) chain system through coordination bonds could generate single-chain magnets (SCMs), a new class of

magnetic materials with Ising-type magnetic anisotropy and strong intrachain magnetic interactions.[4]

Polynuclear Mn clusters have been proven versatile building blocks for constructing SMMs, SCMs and magnetic coordination networks. 1,3-Propanediol derivatives have lead to a variety of Mn aggregates with interesting magnetic properties.[5] In our previous work, we have been able to isolate a linear [$Mn^{II}_2Mn^{III}$] motif as discrete cluster from similar ligand systems. Through modifications on the backbone group of diol ligands, such high spin building units can be assembled into 1D chains through end-to-end azido bridges, with fine control over the alignment of neighbour Mn^{III} Jahn-Teller axes. [6] Layered or tubular aggregates also can be obtained from sulfamide functionalized 1,3-diol ligands and dicyanamide bridges. [7] Although the intratrimer ferromagnetic interactions and the S_T = 7 spin ground state of the [$Mn^{II}_2Mn^{III}$] cluster were preserved during the self-assembling, the magnetic interactions between [$Mn^{II}_2Mn^{III}$] units are *usually* antiferromagnetic, which somewhat prohibits the observation of more exciting magnetic behaviours such as SCM or long range magnetic ordering at higher temperatures. As an extension of our previous work, we sought to prepare ferromagnetically coupled [$Mn^{II}_2Mn^{III}$] networks. Herein, we report the crystal structures and the magnetic properties of a discrete cluster and a ferromagnetic chain based on ferromagnetic [$Mn^{II}_2Mn^{III}$] building unit.

Experimental Section

Materials and Methods

All chemicals were of commercial origin without further purification. *Caution! Although no such tendency was observed during the present work, azide salts are potentially explosive and should be handled with care and in small quantities.*

The magnetic measurements were carried out with a Quantum Design MPMS-XL7 SQUID magnetometer using polycrystalline sample. Magnetic susceptibility data were conducted from 300 to 2 K at 1000 Oe dc field and field-dependant magnetization plots were performed between 2 and 4 K for applied fields ranging from 0 to 70 kOe. The ac susceptibility measurements were conducted with an oscillating ac field of 3 Oe and ac frequencies of 97 and 997 Hz at 0 Oe and 1000 Oe dc fields. Diamagnetic correction has been calculated from Pascal constants and the background of sample holder was also subtracted. Elemental analysis (C, H, and N) was carried out on a Perkin-Elmer 2400 Elemental Analysis. IR spectra were recorded in the range 400-4000 cm^{-1} on a Bruker IFS 66v/S IR spectrometer using KBr pellets. Single-crystal X-ray diffraction measurements of both compounds were carried out on a Rigaku-RAPID diffractometer equipped with graphite-monchromatic MoKα radiation (λ = 0.71073 Å). Absorption corrections were applied by using SADABS. The structures of **1** and

2 were solved by direct methods and refined by full-matrix least-squares techniques based on F^2 using the SHELXS-97 program. All the non-hydrogen atoms were refined with anisotropic parameters. It is noted that the hydrogen atoms were not added to the H_2O in compound **1** as the water molecule is disordered with azide. Crystallographic data have been deposited with the Cambridge Crystallographic Data Centre: CCDC 1025567 for **1** and 1019982 for **2**. Detailed bond length and bond angles are summarized in Table S1 and S2. The selected crystal parameters, data collection, and refinements are summarized in Table 1.

Compound	**1**	**2**
Molecular Formula	$C_{40}H_{64}O_{12}N_2Mn_3Br_5$	$C_{35}H_{46}N_5O_8Mn_3Br_4$
Fw (g mol^{-1})	1329.30	1149.23
Crystal system	Triclinic	Triclinic
Space group	*P*−1	*P*−1
a (Å)	7.8658(16)	8.5966(2)
b (Å)	12.814(3)	11.893(2)
c (Å)	13.709(3)	12.358(3)
α (deg)	86.61(3)	73.30(3)
β (deg)	87.84(3)	75.79(3)
γ (deg)	74.27(3)	73.84(3)
V (Å^3)	1327.3(5)	1143.4(4)
Z	1	1
D (calcd, g cm^{-3})	1.663	1.669
μ (mm^{-1})	4.520	4.360
F(000)	664	570.0
Goodness-of-fit on F^2, *S*	1.046	1.025
R_1, wR_2 [$I \geq 2\sigma(I)$]	0.0616, 0.1697	0.0652, 0.1931
R_1, wR_2 [all data]	0.0962, 0.1968	0.1078, 0.2243

Synthesis

Preparation of 2-[(9H-fluoren-9-yl)amino] propane-1, 3-diol (H_2L):

To a solution of serinol (20 mmol) in THF (80 ml), K_2CO_3 (23 mmol,) was added followed by corresponding electrophiles dropwise of 9Br-fluorene (20 mmol) in 20ml THF at 0 K. Then the reaction mixture was heated for 10h under reflux. After completion of the reaction, THF was removed in vacuo and acetone (100ml) was added to form the precipate, which was removed by filtration. The filtrate was concentrated under reduced pressure. The crude product was purified by column chromatography on silica gel eluted by ethyl acetate, yield: 80%.

Preparation of $Mn_3(HL)_2(CH_3OH)_6(Br)_4 \cdot Br \cdot (CH_3OH)_2$ (**1**)**:**

A solution of $MnBr_2$ $4H_2O$ (0.18 g, 0.6 mmol) in CH_3OH (5 mL) was added with stirring to a solution of H_2L (0.1 g, 0.4 mmol) in CH_3CN (5mL). After the mixture had been stirred for 1 h, the yellow-brown suspension was filtered, and the filtrate was layered by hexane. After 6 days, yellow prism crystals were obtained in c.a. 50% yield (based on Mn). Elemental analysis (%) Calcd for $Mn_3(HL)_2(CH_3OH)_6(Br)_4 \cdot Br \cdot (CH_3OH)_2$ (**1**$\cdot$ 2 CH_3OH) ($C_{40}H_{64}O_{12}N_2Mn_3Br_5$) : C 36.14, H 4.85, N 2.11; found: C 36.02, H 4.78, N 2.02. Selected IR data (KBr pellet): 3355(s), 1593(s), 1448(m), 1410(m), 1118(m), 1068(s), 964(m), 816(w), 737(s), 590(s).

Preparation of $Mn_3(HL)_2(CH_3OH)_2(Br)_4(N_3)(H_2O) \cdot CH_3OH$ (**2**)**:**

A solution of NaN_3 (0.02g, 0.2mmol) in CH_3OH (5 mL) was added with stirring to a solution of $MnBr_2$ $4H_2O$ (0.18 g, 0.6 mmol) and H_2L (0.1 g, 0.4 mmol) in CH_3CN (5mL). After the mixture had been stirred for 1 h, the yellow-brown suspension was filtered, and the filtrate was layered by hexane. After 4 days, light yellow prism crystals were obtained in c.a. 40% yield (based on Mn). Elemental analysis (%) Calcd for $Mn_3(HL)_2(CH_3OH)_2(Br)_4(N_3)(H_2O) \cdot CH_3OH$ (**2** $\cdot$ CH_3OH) ($C_{35}H_{46}N_5O_8Mn_3Br_4$): C 36.58, H 4.03, N 6.09; found: C 36.33, H 4.08, N 6.08. Selected IR data (KBr pellet): 3525(w), 3444(w), 3298(m), 2080(s), 1454(m), 1116(s), 1070(s), 742(m), 548(m).

Results and Discussion

Crystal structure of $Mn_3(HL)_2(CH_3OH)_6(Br)_4 \cdot Br \cdot (CH_3OH)_2$ (**1**)

Single-crystal X-ray diffraction analysis reveals that compound **1** crystalize in the *P*-1 triclinic space group. Crystallographic details on these compounds are summarized in Table 1 and the main bond distances and angles are given in Tables S1 and S2. Compound **1** can be viewed as linear [$Mn^{II}_2Mn^{III}$] trimer containing two Mn^{II} and one Mn^{III} ions, which are linked by two deprotonated diol ligands through the alkoxy

oxygens (Figure 1, left). Each Mn^{II} ions is octahedrally coordinated to two oxygens from two diol ligands, three CH_3OH and one Br^- ion. The central Mn^{III} ion is coordinated to four oxygens from diol ligands and two Br^-, with the much elongated Mn-Br distance of 2.9151(9)Å. Both Br^- ions connect with terminal CH_3OH from Mn^{II} through Hydrogen bonds with the O-Br distance ranging from 3.16 to 3.20Å. The guest molecules include two CH_3OH and one Br^- counter-ion. It should be noted that there are Hydrogen bonds between guest molecules but no detectable weak interactions between the $[Mn^{II}_2Mn^{III}]$ trimers.

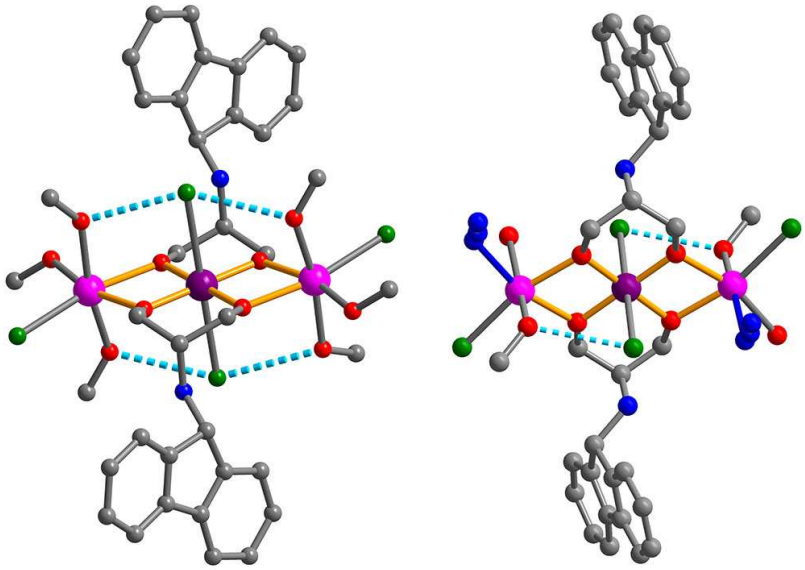

Figure 1: Linear $[Mn^{II}_2Mn^{III}]$ units in **1** (left) and **2** (right). Light blue dashed lines highlight intratrimer H-bonds. (C: grey, Mn^{II}: pink, Mn^{III}: purple; O: red; Br: green; N: blue; H atoms and guest molecules are omitted for clarity).

Crystal structure of $Mn_3(HL)_2(CH_3OH)_2(Br)_4(N_3)(H_2O) \cdot CH_3OH$ (**2**)

Compound **2** crystalize in the *P*-1 triclinic space group. Crystallographic details on these compounds are summarized in Table 1 and the main bond distances and angles are given in Tables S1 and S2. The structure of **2** can be viewed as neutral chains of repeating $[Mn^{II}_2Mn^{III}]$ units linked by means of disordered end-on azido/H_2O bridges (Figure 2). The asymmetric unit of **2** is shown in Figure 1. Similar to our previously results, [6,7] two fully deprotonated diol ligands bridge two Mn^{II} and one Mn^{III} ions through the alkoxy oxygens to form an almost linear $[Mn^{II}_2Mn^{III}]$ unit (Figure 1, right). Each Mn^{II} ion is octahedrally coordinated to two oxygens from two different diol ligands, azide/H_2O, one terminal CH_3OH and one Br^- ion. The central Mn^{III} ions is coordinated to four oxygens from diol ligands and two Br^-, the later define the

orientation of Jahn-Teller axe by elongated Mn-Br bond distance (2.9028(12)Å). Note that both terminal CH_3OH molecules form strong OH-Br bonds with two central Br^- ions (with the O-Br distance of 3.19Å) stabilize the linear trinuclear motif. The $[Mn^{III}Mn^{II}_2L_2X_4]^+$ units are linked into 1D chain through double end-on azido bridges (Figure 2), with the Mn^{III} Jahn-Teller axes are parallel along the chain. Those 1D aggregates are further reinforced in the lattice by intrachain Hydrogen bonds and interchain π–π interactions. (Figure 3) Introduction of different linkers such as dicyanamide to connect this $[Mn^{II}_2Mn^{III}]$ motif into different networks failed, however, further modification of the diol ligand and variation of the counter ions might allow us to obtain other possible coordination networks based on the same building block.

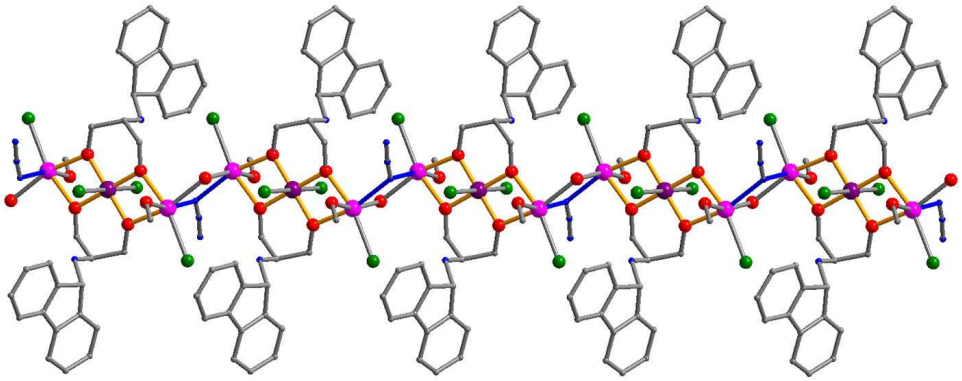

Figure 2: 1D chain structure of **2** based on $[Mn^{II}_2Mn^{III}]$ units linked by means of disordered end-on azido/H_2O bridges.

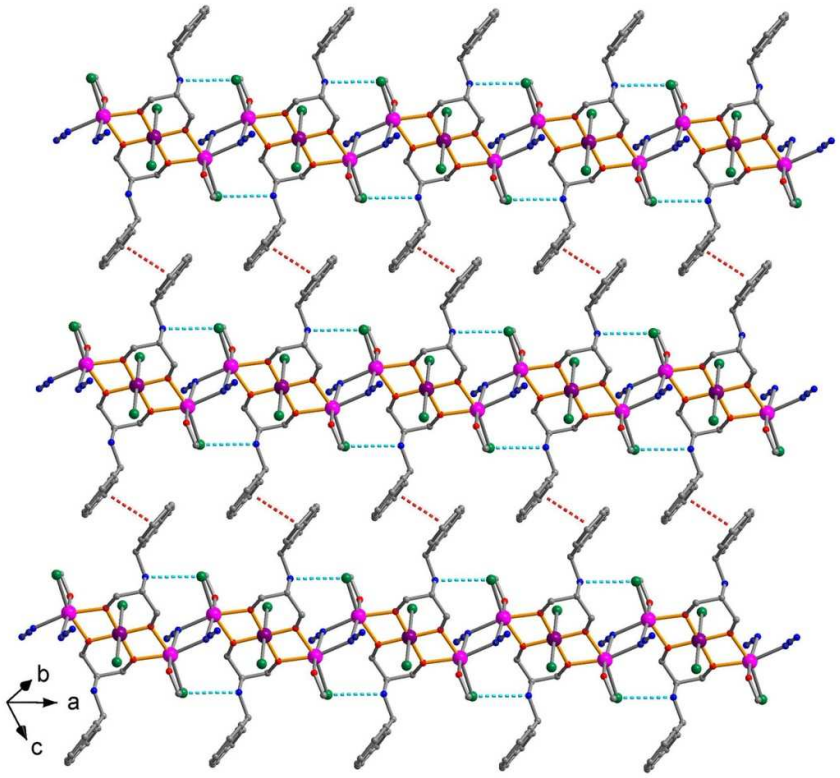

Figure 3: 2D supramolecular aggregates of **2** linked by intrachain hydrogen bonds (light blue dashed lines) and interchain π–π interactions (red dashed lines).

Magnetic properties

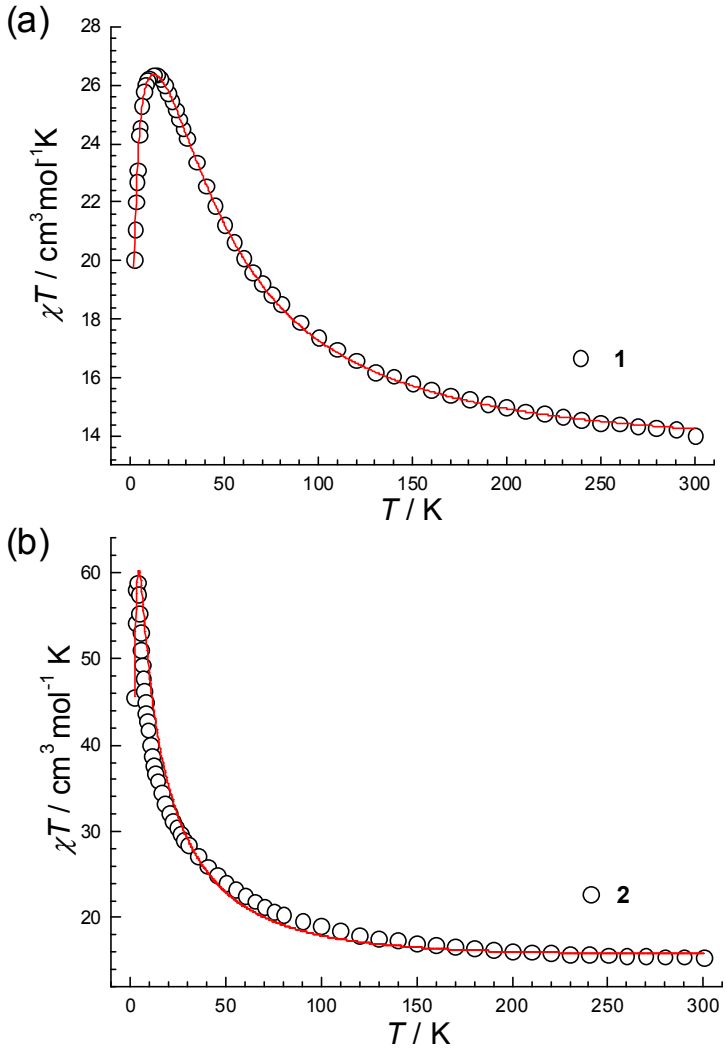

Figure 4: (a) χT *vs.* T plot under 1000 Oe dc field for **1**; (b) χT *vs.* T plot under 1000 Oe dc field for **2**. The red lines represent the fitting curves.

The magnetic behaviours of **1** and **2** were studied on polycrystalline samples. Temperature-dependent magnetic susceptibility data were measured between 2 and 300 K under 1000 Oe dc field (Figure 4). At room temperature, the χT products for **1** and **2** are 14.0 and 15.4 cm^3 K mol^{-1}, respectively, which are both higher than the theoretical spin-only value per [$Mn^{III}Mn^{II}_2$] unit (*calcd.* 11.75 cm^3 K mol^{-1} for $S_{Mn(III)}$ = 2, $S_{Mn(II)}$= 5/2 and $g_{Mn(III)}$ = $g_{Mn(II)}$ = 2), indicating ferromagnetic interactions in both compounds. Upon cooling, χT vs. T curves display different behaviours for the two compounds. For **1**, χT increases gradually and exhibit a broad peak with a maximum of 26.4 cm^3 K mol^{-1} at 14 K, corresponding to the S_T = 7 ground state for isolated [$Mn^{II}_2Mn^{III}$] unit. The further decrease of χT below 14 K ascribes to the antiferromagnetic intermolecular interactions. Based on the trimer structure, the

magnetic susceptibility was fitted by the following Hamiltonian: $\hat{H} = -2J(\hat{S}_A\hat{S}_1 + \hat{S}_1\hat{S}_B)$ where J defines the $Mn^{II}\cdots Mn^{III}$ magnetic interaction within the $[Mn^{II}_2Mn^{III}]$ unit. In order to fit the lower temperature data, inter-complex magnetic interactions, J', and temperature-independent paramagnetism (TIP) have been added in the frame of the mean field approximation. [8] The best fitting affords J/k_B = 6.39(8) K, g = 2.04(1), zJ'/k_B = –0.018(1) K, TIP = 0.0013(2). The positive J indicates the dominant intramolecular ferromagnetic interactions. To investigate the magnetic anisotropy of the Mn_3 trimer, a model considering the intra-complex magnetic interaction, J, and the Mn^{III} magnetic anisotropy, D, (defined by the following anisotropy Hamiltonian: $\hat{H}_A = DS^2_{1,z}$) was applied to reproduce the experimental data. However, no physically meaningful D values have been obtained. Ac susceptibility measurements were performed below 15 K and shown the complete absence of out-phase signal above 1.8 K, which is coincident with the previously reported Mn_3 trimer with similar linear $[Mn^{II}\text{-}Mn^{III}\text{-}Mn^{II}]$ motif, [6, 9] indicating the negligible magnetic anisotropy in **1**.

For compound **2**, the χT keeps a roughly constant when the temperature went down to 150 K followed by a gradual increase to 50 K. Afterwards, an abrupt increase was observed with a distinct sharp peak of 58.9 cm^3 K mol^{-1} at 3.5 K. This peak value is much higher than the excepted value for isolated $[Mn^{II}_2Mn^{III}]$ unit with S_T = 7, highlighting the ferromagnetic intertrimer interactions mediated by the end-on azido/H_2O bridges between Mn^{II} metal ions. Below 3.5 K, the decrease of the χT product might be the results of the saturation of the magnetization and/or weak antiferromagnetic interchain interactions, likely mediated by π–π stacking. On the basis of the crystal structures, the magnetic susceptibility of this 1D compound was modeled using the following Hamiltonian, $\hat{H} = -2\sum_{i=1}^{N} J_1(\hat{S}_{A,i}\hat{S}_{1,i} + \hat{S}_{1,i}\hat{S}_{B,i}) + J_2(\hat{S}_{B,i}\hat{S}_{A,i+1})$ where J_1 is the $Mn^{II}\cdots Mn^{III}$ magnetic interaction within the $[Mn^{II}_2Mn^{III}]$ unit and J_2 represents the $Mn^{II}\cdots Mn^{II}$ magnetic interaction through the disordered end-on azido/H_2O linkers. [10] In order to fit the lower temperature data, mean field approximation zJ'' that describes the inter-chain magnetic interactions and temperature-independent paramagnetism (TIP), were also added to the model. [8] As shown in Figure 4, the best fit of the data is obtained with J_1/k_B = +5.5(3) K, J_2/k_B = +0.61(3) K, g = 2.05(1), zJ''/k_B = –0.029(8) K and TIP = 0.0068(8). The estimation of the intratrimer $Mn^{II}\cdots Mn^{III}$ interaction (J_1) is in excellent agreement with our previously results.[6] Weak ferromagnetic coupling between Mn^{II} ions is anticipated

through end-on azido bridges as the Mn–N–Mn bridge angles are appreciably less than 104°,[11] an angle that separates the ferro- and antiferro- magnetic interactions in end-on bridged azido system. In **2**, the corresponding angle is 101.1° and the resulted J_2 value is well consistent with other reported values. [12] Thus, **2** can be magnetically described as a ferromagnetic chain of ferromagnetic [$Mn^{II}_2Mn^{III}$] trimers.

Ac susceptibility measurements were performed below 15 K and show complete absence of out-of-phase (Figure S1) signal above 2 K even under a static field of 0.1 T. The absence of slow-magnetic relaxation behaviour for **2**, in spite of the ferromagnetic intertrimer interactions and the parallel assignment of the Mn^{III} Jahn-Teller, is likely due to the very small magnetic anisotropy of [$Mn^{II}_2Mn^{III}$] unit. It's also possible that the global anisotropy is quenched by interchain weak interactions such as π–π interactions.

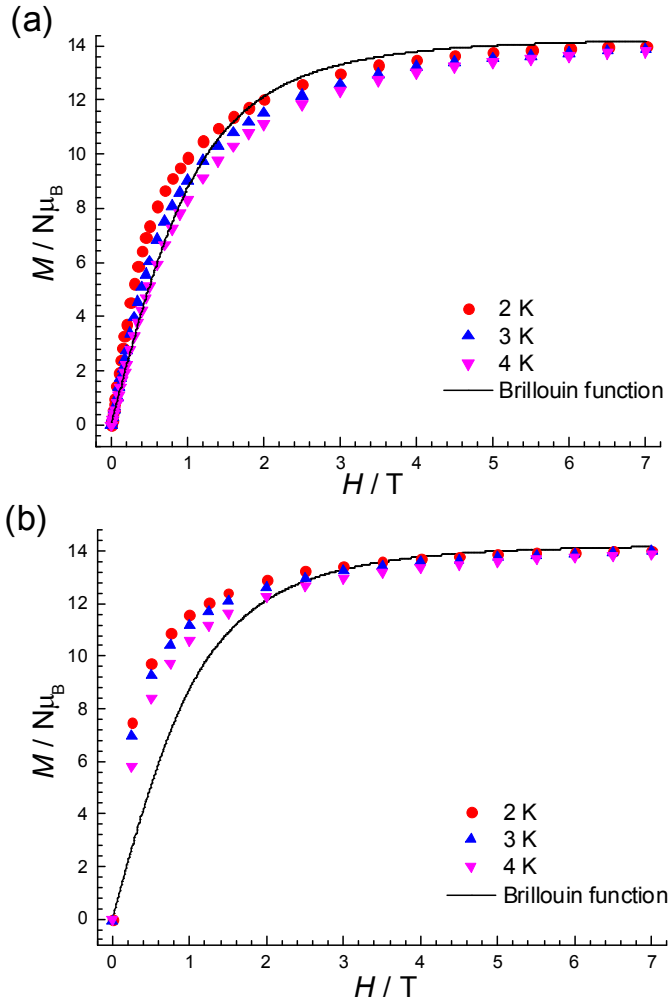

Figure 5: Isothermal magnetization curves for **1** (a) and for **2** (b) collected from 2 K to 4 K. The black lines are calculated Brillouin function for the $[Mn^{II}_2Mn^{III}]$ unit at T = 2 K with $g(Mn^{II})$ = 2.05 and $g(Mn^{III})$ = 1.98.

The isothermal magnetization plots for **1** and **2** at variable fields at low temperatures were also conducted. As shown in Figure 5, the magnetization (M) rises quickly at low fields and reaches 13.98 and 14.03 μ_B at 7 T at 2 K for two compounds, respectively, which are the expected saturated value considering two S = 5/2, g = 2.05 and one S = 2, g = 1.98 centers (14.15μ_B). The Brillouin function was also performed using the above parameters at 2 K. The obvious larger magnetization values at low temperature (e.g. 2 K) than the Brillouin functions for **2** clearly confirm that all the intra- and inter-$[Mn^{II}_2Mn^{III}]$ trimer interactions are ferromagnetic.

Conclusions

In this work, we report a discrete cluster and a ferromagnetic chain based on ferromagnetic $[Mn^{II}_2Mn^{III}]$ building unit. The structural and magnetic studies indicate that the ferromagnetic nature of the $[Mn^{II}_2Mn^{III}]$ trimer remains unchanged in both discrete and polymeric assembles. These results indicate that the magnetic interactions between the $[Mn^{II}_2Mn^{III}]$ trimer could be fine controlled by careful selection of the 1,3-diol ligand functionality and the bridging linkers. The stability of the $[Mn^{II}_2Mn^{III}]$ motif as building blocks could allow us to imagine other possible coordination networks of higher dimensionalities with more exciting magnetic properties.

Acknowledgements

The authors thank the National Natural Science Foundation of China (21471066, 21390394, 21261130584, 91022030, 21201137), the National Basic Research Program of China (2012CB821700, 2011CB808703), “111” project (B07016), Award Project of KAUST (CRG-1-2012-LAI-009) and Ministry of Education, Science and Technology Development Center Project (20120061130012).

Notes and references

[a] State Key Laboratory of Inorganic Synthesis & Preparative Chemistry, Jilin University, 2699 Qianjin Street, Changchun 130012 (P. R. China)

[b] Centre for Applied Chemical Research, Frontier Institute of Science and Technology, Xi'an Jiaotong University, Xi'an 710054, China

Electronic Supplementary Information (ESI) available: [details of any supplementary information available should be included here]. See DOI: 10.1039/b000000x/

(1) (a) R. Sessoli, D. Gatteschi, A. Caneschi, M. A. Novak, *Nature*, 1993, **365**, 141. (b) G. Christou, D. Gatteschi, D. N. Hendrickson, R. Sessoli, *MRS Bull.* 2000, **25**, 66. (c) M. Leuenberger, D. Loss, *Nature* 2001, **410**, 789. (d) D. Gatteschi, R. Sessoli, *Angew. Chem., Int. Ed.* 2003, **42**, 268. (e) G. Aromi, E. K. Brechin, *Struct. Bonding* (Berlin) 2006, **122**, 1. (f) D. Gatteschi, R. Sessoli, J. Villain, *Molecular Nanomagnets*; Oxford University Press: Oxford, U.K., **2006**. (g) Y. Z. Zheng, G. J. Zhou, Z. Zheng and R. E. P. Winpenny, *Chem. Soc. Rev.*, 2014, **43**, 1462. (h) Y.-Z. Zheng, Z. Zheng, X.-M. Chen, *Coord. Chem. Rev.*, 2014, **258-259**, 1.

(2) For recent views, please see: (a) H. Miyasaka and M. Yamashita, *Dalton Trans.*, 2007, 399. (b) H.-L. Sun, Z.-M. Wang and S. Gao, *Coord. Chem. Rev.*, 2010, **254**, 1081. (c) I-R. Jeon, R. Clérac, *Dalton Trans.,* 2012, **41**, 9569. (d) K. S. Pedersen, J. Bendix, R Clérac, *Chem. Commun.* 2014, **50**, 4396; and the references therein.

(3) (a) W. Wernsdorfer,; N. Aliaga-Alcalde, D. N. Hendrickson, G. Christou, *Nature* 2002, **416**, 406. (b) R. Tiron, W. Wernsdorfer, N. Aliaga-Alcalde, G. Christou, *Phys. Rev. B* 2003, **68**, 140407.

(4) (a) A. Escuer, G. Vlahopoulou, F. A. Mautner, *Inorg. Chem.* 2011, **50**, 2717. (b) Y.-Z. Zheng, L. Qin, Z. Zheng, X.-M. Chen, *Dalton Trans.*, 2013, **42**, 1770. (c) L. Qin, Z. Zhang, Z. Zheng, M. Speldrich, P. Kögerler, W. Xue, B.-Y. Wang, X.-M. Chen, Y.-Z. Zheng, *Dalton Trans.*, 2014, DOI: 10.1039/c4dt02599g.

(5) (a) Moushi, E. E.; Stamatatos, T. C.; Wernsdorfer, W.; Nastopoulos, V.; Christou, G.; Tasiopoulos, A. J. *Angew. Chem. Int. Ed.* **2006**, *45*, 7722. (b) Moushi, E. E.; Lampropoulos, C.; Wernsdorfer, W.; Nastopoulos, V.; Christou, G.; Tasiopoulos, A. J. *Inorg. Chem.* **2007**, *46*, 3795. (c) Moushi, E. E.; Masello, A.; Wernsdorfer, W.; Nastopoulos, V.; Christou, G.; Tasiopoulos, A. J. *Dalton Trans.* **2010**, *39*, 4978. (d) Nayak, S.; Beltran, L. M. C.; Lan, Y.; Clérac, R.; Hearns, N. G. R.; Wernsdorfer, W.; Anson, C. E.; Powell, A. K. *Dalton Trans.* **2009**, 1901. (e) Moushi, E. E.; Lampropoulos, C.; Wernsdorfer, W.; Nastopoulos, V.; Christou, G.; Tasiopoulos, A. J. *J. Am. Chem. Soc.*, **2010**, *132*, 16146. (f) Wu, G.; Huang, J.; Sun, L.; Bai, J.; Li, G.; Cremades, E.; Ruiz, E.; Clérac, R.; Qiu, S. *Inorg. Chem.* **2011**, *50*, 8580. (g) Charalambous, M.; Moushi, E. E.; Constantina Papatriantafyllopoulou, C.; Wernsdorfer, W.; Nastopoulos, V.; Christou, G.; Tasiopoulos, A. J. *Chem. Commun.*, **2012**, *48*, 5410. (h) Moushi, E. E.; Stamatatos, T. C.; Nastopoulos, V.; Christou, G.; Tasiopoulos, A. J. *Polyhedron*, **2009**, *28*, 1814.

(6) J. Huang, G. Wu, J-Q. Bai, Y. Jiang, G-H. Li, S-L. Qiu, R. Clérac, R. *Inorg. Chem.* 2013, **52**, 11051.

(7) G. Wu, J-Q. Bai, Y. Jiang, G-H. Li, J. Huang, Y. Li, C. E. Anson, A. K. Powell, S-L. Qiu, *J. Am. Chem. Soc.* 2013, **135**, 18276.

(8) (a) C. J. O'Connor, *Prog. Inorg. Chem.* 1982, **29**, 203; (b) B. E. Myers, L. Berger, S. Friedberg, *J. Appl. Phys.* 1969, **40**, 1149.

(9) A. Prescimone, J. Wolowska, G. Rajaraman, S. Parsons, W. Wernsdorfer, M. Murugesu, G. Christou, S. Piligkos, E. J. L. McInnes, E. K. Brechin. *Dalton Trans.* **2007**, 5282.

(10) M. E. Fisher, *Am. J. Phys.* 1964, **32**, 343.

(11) (a) A. Escuer, J. Esteban, S. P. Perlepes, T. C. Stamatatos *Coord. Chem. Rev.* 2014, **275**, 87; (b) E. Ruiz, J. Cano, S. Alvarez, P. Alemany, *J. Am. Chem. Soc.* 1998, **120**, 11122.

(12) (a) Abu-Youssef, M. A. M.; Escuer, A.; Gatteschi, D.; Goher, M. A. S.; Mautner, F. A.; Vicente, R. *Inorg. Chem.,* **1999**, 38, 5716. (b) Manson, J. L.; Arif, A. M.; Miller, J. S. *Chem. Commun.*, **1999**, 1479. (c) Karmakar, T. K.; Ghosh, B. K.; Usman, A.; Fun, H.-K.; Rivière, E.; Mallah, T.; Aromì G.; Chandra, S. K. *Inorg. Chem.*, **2005**, 44. 2391.

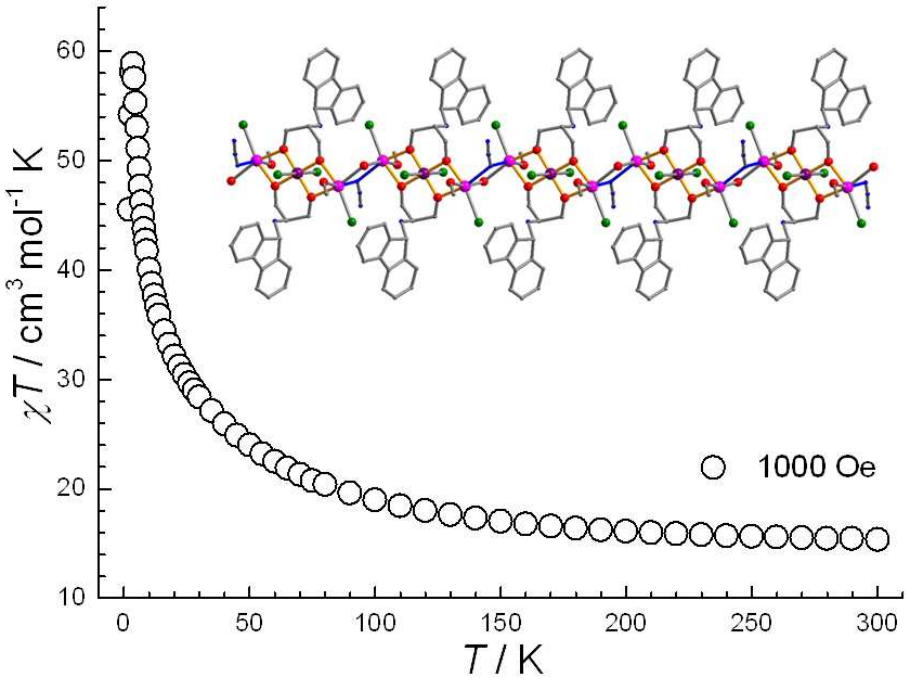

A ferromagnetic chain based on a [Mn_3] ferromagnetic building block is reported.